biomolecules

MDPI

Article

DNA Methylation and Epiallele Diversity in Cord Blood from Newborns Conceived Through Assisted Reproductive Technology: An Exploratory Study

Michihiro Yamamura [1,†], Tomoko Kawai [2,†], Kazuhiko Nakabayashi [2], Kosuke Taniguchi [2,3], Osamu Samura [1] and Kenichiro Hata [2,3,*]

[1] Department of Obstetrics and Gynecology, The Jikei University School of Medicine, Tokyo 105-8461, Japan; osamusamura@gmail.com (O.S.)
[2] Department of Maternal-Fetal Biology, National Center for Child Health and Development, Tokyo 157-8535, Japan; kawai-tm@ncchd.go.jp (T.K.); nakabaya-k@ncchd.go.jp (K.N.); taniguchi-k@gunma-u.ac.jp (K.T.)
[3] Department of Medical Genetics and Genomics, Gunma University Graduate School of Medicine, Gunma 371-8511, Japan
* Correspondence: khata@gunma-u.ac.jp
† These authors contributed equally to this work.

Abstract

Background: Studies of offspring DNA methylation following assisted reproductive technology (ART) have largely focused on mean methylation. We explored epiallele diversity as a complementary measure. Methods: Reduced representation bisulfite sequencing was performed on umbilical cord blood from 87 newborns conceived naturally, through in vitro fertilization, or intracytoplasmic sperm injection (ICSI). Analyses included 287,027 CpGs and mean methylation in 25 predefined imprinted differentially methylated regions (DMRs). Epipolymorphism was calculated from four-CpG blocks in 24 DMRs. Models were adjusted for sex, parity, and maternal pre-pregnancy body mass index. Results: No CpG was significant after false discovery rate (FDR) correction. ICSI was associated with lower weighted mean methylation at PRR25 (adjusted difference, −13.0 percentage points; 95% confidence interval, −19.7 to −6.4; FDR-adjusted $p < 0.01$), and the association remained significant in most sensitivity analyses. No epipolymorphism difference remained significant after FDR correction in the primary analysis. At PRR25, the nominally lower epipolymorphism was closely related to lower mean methylation and did not establish an independent change in epiallele diversity. Conclusions: This exploratory study identified an ICSI-associated methylation difference at PRR25 and applied epipolymorphism to complement mean-based assessment of neonatal methylation. The findings support evaluating these measures together, while independent validation is needed.

Keywords: assisted reproductive technology; DNA methylation; epiallele diversity; epipolymorphism; genomic imprinting; reduced representation bisulfite sequencing

Check for updates

Academic Editor: Haengseok Song

Received: 19 October 2026
Revised: 13 November 2026
Accepted: 18 November 2026
Published: 25 November 2026

Copyright: © 2026 by the authors. Licensee MDPI, Basel, Switzerland. This article is an open access article distributed under the terms and conditions of the Creative Commons Attribution (CC BY) license.

1. Introduction

Changes in the epigenome in response to environmental factors may contribute to disease susceptibility [1]. In assisted reproductive technology (ART), gametes and early embryos are exposed to an in vitro environment during a critical period of epigenomic reprogramming. Accordingly, concerns have been raised about the potential impact of ART on the offspring epigenome.

Early case series suggested that children conceived by ART might have a higher frequency of imprinting disorders than the general population. Subsequent meta-analyses have also reported an association between ART conception and an increased risk of imprinting disorders [2,3]. However, the extent to which ART procedures contribute to this association, rather than parental infertility or other background factors, remains uncertain.

Environmental stress can be associated with widespread epigenetic alterations as well as changes at specific genomic loci [4]. ART-related exposures, including in vitro culture and embryo manipulation, can occur during early development, from fertilization to the blastocyst stage. If these exposures induce epigenetic changes, such changes may be distributed heterogeneously among cells.

Previous studies using blood samples from newborns have examined between-group differences in DNA methylation levels at CpG sites across the genome and within imprinted regions [5,6]. Birth-cohort epigenome-wide association studies (EWAS) have yielded varying findings regarding ART-associated methylation differences [7–9]. These analyses have generally focused on between-group differences in methylation levels measured in bulk samples. However, identical mean methylation levels can arise from different underlying distributions of methylation patterns, which cannot be distinguished by mean values alone.

Epipolymorphism analysis has been used to characterize epiallele diversity and DNA methylation heterogeneity in tumor tissues [10,11]. By quantifying the distribution of methylation patterns across sequencing reads at a given locus, this approach provides information complementary to mean methylation levels.

Accordingly, in this study, we used reduced representation bisulfite sequencing (RRBS) to examine mean DNA methylation levels and epiallele diversity in umbilical cord blood from newborns conceived naturally or through ART. Epipolymorphism was included as an exploratory measure to complement mean-based analyses. Umbilical cord blood was selected because sampling at birth limits the influence of postnatal environmental exposures.

2. Materials and Methods

2.1. Sample Collection

Participants were selected from the institutional perinatal biobank at the National Center for Child Health and Development. Pregnant women attending prenatal care were recruited during January 2011 and September 2015. The method of conception was ascertained from both questionnaire and medical records. This analysis included mother–infant pairs with singleton infants born at term following pregnancies and deliveries without apparent complications. Mothers had no apparent underlying disease, and no apparent disease or abnormality was identified in the offspring prenatally, at birth, or through the one-month checkup. Women with underlying medical conditions requiring pharmacological treatment were excluded. Maternal smoking and alcohol consumption during pregnancy were exclusion criteria. Medication use for the management of common pregnancy-related symptoms or minor intercurrent illnesses was not, in itself, an exclusion criterion.

The candidate pool considered for this analysis comprised 350 mother–infant pairs in the NC group, 72 in the IVF group, and 67 in the ICSI group. After applying these eligibility criteria, we selected 30 newborns in each conception group (NC, IVF, and ICSI), with the aim of obtaining similar distributions of maternal age at delivery and gestational age at delivery across the three groups. Following sequencing quality control, one sample from each group was excluded, leaving 87 newborns (29 per group) in the final analysis. Their characteristics are summarized in Table 1.

Statistical comparisons of between-group characteristics were performed using the Student's *t*-test for continuous variables and the chi-square test for categorical variables.

All analyses were conducted using R software (version 4.3.1, R Foundation for Statistical Computing, Vienna, Austria).

Table 1. Characteristics of the study participants.

	NC (n = 29)	IVF (n = 29)	ICSI (n = 29)
Maternal age at delivery, mean (SD)	37.8 (3.3)	38.4 (3.1)	38.6 (3.2)
Paternal age at delivery, mean (SD)	38.8 (3.6) (n = 26)	40.0 (4.0) (n = 25)	40.2 (3.3) (n = 28)
Maternal pre-pregnancy BMI, mean (SD)	20.7 (1.0)	19.7 (1.7) *	20.4 (1.3)
Maternal parity, No. (%)			
Primipara	13 (44.8)	26 (89.7) *	22 (75.9) *
Multiparous	16 (55.2)	3 (10.3)	7 (24.1)
Child birthweight, mean (SD)	3088 (248)	3009 (340)	3175 (330)
Child gestational age, mean (SD)	39.5 (1.0)	39.3 (1.3)	39.8 (1.2)
Child sex, No. (%)			
Male	15 (51.7)	11 (37.9)	16 (55.2)
Female	14 (48.3)	18 (62.1)	13 (44.8)

Values are presented as mean (SD) or number (%), based on the 87 newborns included in the final analysis (29 per group). For paternal age, the number of participants with non-missing data (n) is indicated separately for each group. Percentages are calculated using the number of participants with available data as the denominator. NC, natural conception; IVF, in vitro fertilization; ICSI, intracytoplasmic sperm injection; SD, standard deviation; BMI, body mass index. * p values < 0.05 were considered statistically significant. Chi-square tests were used for categorical variables and two-sided t-tests for continuous variables.

2.2. DNA Preparation

At birth, 5 mL of umbilical cord blood was collected from the umbilical vein (Figure 1). Genomic DNA was extracted from whole blood samples using the standard protocol of the QIAsymphony DNA Midi kit (Qiagen, Hilden, Germany).

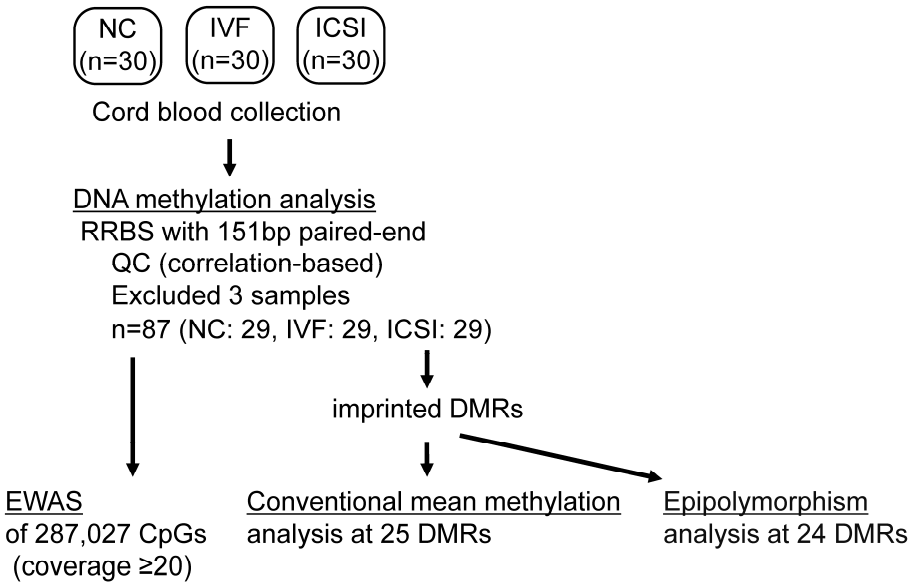

Figure 1. Study Overview. Note: NC, Natural Conception; IVF, In Vitro Fertilization; ICSI, Intracytoplasmic Sperm Injection; RRBS, Reduced Representation Bisulfite Sequencing; DMR, Differentially methylated region; EWAS, Epigenome-Wide Association Study.

2.3. Reduced Representation Bisulfite Sequencing (RRBS)

Reduced-representation bisulfite sequencing libraries were prepared as previously described [12–14]. Briefly, 100 ng of genomic DNA was digested with 20 units of MspI (Thermo Scientific, ER0542, Waltham, MA, USA), using the NEBNext UltraII DNA Library Prep Kit (NEB, E7645) with xGen Methyl UDI-UMI Adapters (IDT). Bisulfite conversion was performed with the EZ DNA Methylation-Gold Kit (Zymo Research, Irvine, CA, USA), followed by nine cycles of PCR amplification. No size selection was performed at any stage of library preparation; the entire MspI digestion product was carried through to sequencing, and the resulting insert size distribution is reported below and in Table S1. Libraries were sequenced on the HiSeq X Ten (Illumina, San Diego, CA, USA), generating 2 × 151 bp paired-end reads.

The xGen UDI-UMI adapters have a Y-adapter orientation that is inverted relative to conventional Illumina adapters. Consequently, in the delivered FASTQ files, read 1 begins at the end-repair fill-in bases and read 2 begins at the MspI cleavage site. The two mates were exchanged before trimming so that read 1 corresponded to the MspI-derived end, as assumed by RRBS-aware tools. The exchange was verified by inspecting the trinucleotide composition at the 5′ end of each mate before and after trimming; read 1 was enriched for CGG/TGG and read 2 for CAA, as expected. Although the libraries were prepared with UMI-containing adapters, the UMI sequences were not present in the delivered reads and were not used in the analysis.

Reads were trimmed with Trim Galore v0.6.6 (cutadapt v3.2) using –rrbs –paired –illumina –quality 20 –phred33 –stringency 1 -e 0.1 –length 20. The –rrbs option removes 2 bp from the 3′ end of adapter-trimmed read 1 and 2 bp from the 5′ end of read 2 (equivalent to –clip_r2 2), thereby excluding cytosines introduced during MspI end-repair/fill-in. Read pairs in which either mate fell below 20 bp after trimming were discarded.

Trimmed reads were aligned to the hs37d5 reference with Bismark [15] v0.22.3 and Bowtie2 [16] v2.0.6 using –non_directional, which searches all four bisulfite strands without assuming a strand of origin. This setting was adopted because of the inverted adapter orientation. All other parameters were left at their Bismark v0.22.3 defaults. Only read pairs with a unique best alignment were retained. Mapping efficiency was computed as the number of uniquely aligned read pairs divided by the number of input read pairs. The median per-sample mapping efficiency was 77.17% (range, 69.83–79.85%; $n = 90$). Per-library values are given in Table S1.

PCR duplicates were assessed but not removed, since, in RRBS, independently generated molecules can share MspI-defined alignment coordinates, so coordinate-based deduplication can discard genuine molecules.

Methylation calls were extracted with bismark_methylation_extractor -p –comprehensive –merge_non_CpG –bedGraph. In paired-end mode, –no_overlap is enabled by default, so cytosines in the region where the two mates overlap were counted only once, from read 1. No positional masking was applied (–ignore, –ignore_r2, –ignore_3prime, and –ignore_3prime_r2 were all left at 0); M-bias plots showed no position-dependent artifact after mate exchange and RRBS trimming. Genome-wide CpG reports were generated with coverage2cytosine –coverage_threshold 1 (CpG context only, 1-based coordinates, strands not merged) and converted to methylKit input format.

Bisulfite conversion efficiency was estimated from non-CpG cytosines as 100 × unmethylated CH/total CH, where CH denotes the CHG and CHH contexts combined. Because genuine non-CpG methylation is counted as unconverted, this is a conservative lower bound. The median per-sample conversion efficiency was 99.43% (range 99.32–99.55%, $n = 90$). Per-library values are given in Table S1.

Insert sizes were derived from the coordinate-sorted Bismark BAM files without realignment. The absolute value of TLEN was taken from every first-in-pair primary alignment (samtools view -f 64 -F 0 × 900), which counts each read pair exactly once irrespective of mate order, and accumulated into a histogram with 1 bp bins per library; the median, 25th and 75th percentiles were read from the cumulative histogram without interpolation, and the mean was computed as the count-weighted average. The median per-library insert size was 172 bp (range of per-library medians 115–226 bp, $n = 90$). Per-library values are given in Table S1.

Libraries for the 87 analyzed samples were prepared in five batches. Sequencing was performed in six runs. NC and ICSI samples were distributed across the same five runs, whereas 15 of the 29 IVF samples were sequenced in a run without NC samples. Sample allocation by library preparation batch and sequencing run is provided in Table S2.

Since DNA methylation profiles in peripheral blood are influenced by leukocyte composition, cell composition estimation and deconvolution methods have been established for DNA methylation array [17] and whole-genome bisulfite sequencing (WGBS) data [18]. We examined the coverage of 600 CpG markers in the selected published reference panel for cell-type deconvolution [19]. Only 32 of these markers were covered in our RRBS dataset, and we did not obtain reliable cell-composition estimates using this panel. Cell composition was therefore not included in the regression models.

2.4. Epigenome-Wide Association Study (EWAS)

Methylation call files generated by Bismark were analyzed using the R package methylKit (version 1.20.0) [20]. CpGs with read coverage ≥20 in all 87 samples were extracted, and 287,027 CpGs were included in the analysis. For each CpG, separate linear regression models were fitted to compare IVF with NC and ICSI with NC, with DNA methylation level as the dependent variable. NC was the reference group, and the third conception group was excluded from each model. Each comparison included 58 participants (29 per group).

Using the natural conception group (NC) as the reference group, we performed an EWAS [21,22]. In addition to sex, which is a factor influencing DNA methylation, parity and pre-pregnancy body mass index (BMI)—both of which exhibited variations in distribution among the groups in this study (Table 1)—were incorporated into the models as covariates. The Benjamini–Hochberg false discovery rate (FDR) procedure was used to correct for multiple comparisons, with significance defined as an FDR-adjusted p-value < 0.05. Using the p-values theoretically expected under the null hypothesis and the p-values observed from the multiple linear regression models described above, we calculated the genomic inflation factor λ defined by Devlin and Roeder as the median of the observed chi-square statistics divided by the median of the theoretically expected chi-square statistics [23].

The distribution of p-values is also shown using a QQ plot, in which the negative common logarithm of the theoretically expected p-values under the null hypothesis is plotted on the x-axis and the negative common logarithm of the observed p-values from the multiple linear regression models is plotted on the y-axis.

2.5. Mean-Based Methylation Analysis of Imprinted Differentially Methylated Regions (DMRs)

Independently of the EWAS results, we referred to imprinted DMRs defined by previously reported oxidative whole-genome bisulfite sequencing analyses [24] and extracted CpGs located within those DMRs from the RRBS data. We further extracted only CpGs with coverage ≥20 in all 87 samples and ultimately included 25 imprinted DMRs in the analysis (Figure 1, Table S3).

The DNA methylation level of each DMR was calculated by first deriving the methylation level of each CpG and then computing a weighted average using read coverage as the weight. For each DMR, separate linear regression models were fitted with the weighted mean methylation level as the dependent variable, comparing IVF with NC and ICSI with NC. The third conception group was excluded from each comparison. Models were adjusted for offspring sex, maternal parity, and pre-pregnancy BMI. Each mean-methylation comparison included 58 participants (29 per group), with no missing covariate data.

The regression coefficient (COE) represents the difference in the weighted mean methylation level relative to that of the NC group. Ninety-five percent confidence intervals were calculated using the Wald method, and *p*-values were obtained using the Wald *t*-test. Multiple-testing correction is described in Section 2.7.

2.6. Epipolymorphism Analysis of Imprinted DMRs

Methylation patterns were extracted from the aligned BAM files using MethClone (version 0.2; -d 150 -c 20) [25]. MethClone counted each read pair once per block, which we verified by comparing its read counts with the number of read pairs in the aligned BAM files. Four consecutive CpGs within a read defined a block, with a maximum span of 150 bp. Blocks were generated by moving the window one CpG at a time. The compMatrix function in epihet (version 1.6.1; readNumber = 20, $p = 0.8$) [11] retained blocks with at least 20 reads in at least 80% of the 87 samples. These thresholds were chosen to support reliable estimation of epipolymorphism and were more stringent than those used in a previous study (≥10× coverage in ≥75% of samples) [26]. We further restricted the analysis to blocks composed entirely of CpGs included in the mean-methylation analysis, each with coverage ≥20 in all 87 samples. The resulting set comprised 137 blocks in 24 DMRs; MEST had no qualifying block.

For each block, epipolymorphism was calculated as $H = 1 - \Sigma_{i=1}{}^{16}\, p_i{}^2$, where p_i is the proportion of reads with methylation pattern i. In each sample, blocks with fewer than 20 reads were excluded, and the remaining block values were averaged within each DMR using read counts as weights: $H_DMR = \Sigma_b\, n_b\, H_b \,/\, \Sigma_b\, n_b$, where n_b and H_b are the read count and epipolymorphism of block b. No finite-read correction was applied to block epipolymorphism in the primary analysis. In a sensitivity analysis (#8 in Table S7), block values were multiplied by $n/(n-1)$, where n is the number of reads, corresponding to the unbiased correction under independent multinomial sampling. We also used unweighted regional means (#9 in Table S7) and a set of 45 blocks sharing no CpGs (#10; selection procedure in Table S7). These analyses assess sensitivity to the block summary and do not assume that overlapping blocks represent independent observations. Each participant contributed one regional value to each regression. Samples without a qualifying block in a DMR were excluded from that DMR's model, resulting in 52–57 participants per comparison for five DMRs. Block counts and sample sizes for each DMR and comparison are provided in Table S7.

Regional epipolymorphism values were analyzed using the separate adjusted regression models described in Section 2.5. Coefficients represent differences in regional epipolymorphism relative to NC. Confidence intervals and nominal *p*-values were obtained from these models. Multiple-testing correction is described in Section 2.7.

2.7. Model Diagnostics and Sensitivity Analyses

For the regional models, residual distributions were examined using Q–Q plots and Shapiro–Wilk tests, heteroscedasticity using studentized Breusch–Pagan tests, and influential observations using Cook's distance. Sensitivity analyses (#1-#11: Tables S6 and S7) used HC3 heteroscedasticity-consistent standard errors (#1), excluded observations with Cook's

distance >4/n (#2), fitted quasi-binomial generalized linear models (#3), and additionally adjusted for sequencing depth (#4) or library preparation batch (#5). Sequencing run was added to the ICSI–NC models (#5b). Because the IVF and NC groups had limited overlap across runs, the corresponding sensitivity analysis was restricted to runs containing both groups ($n = 30$). To assess the influence of incomplete bisulfite conversion, methylation levels were corrected for the sample-specific non-conversion rate c (100% minus the conversion efficiency; Table S1) as $(M - c)/(1 - c)$, where M is the observed methylation proportion (#7), and the non-conversion rate was added as a covariate (#7b). Maternal age was also added in a sensitivity analysis (#11). Leave-one-out analyses were performed for the PRR25_1 methylation association.

For epipolymorphism, additional models included the mean methylation of the same DMR as a linear term (#6) or as linear and quadratic terms (#6b). Only #7b was performed for epipolymorphism, because correcting epiallele frequencies for non-conversion would require read-level adjustment. Alternative block summaries are described in Section 2.6 (#8-#10). These sensitivity analyses were specified after the initial submission. Model specifications and results are provided in Tables S6 and S7.

The Benjamini–Hochberg procedure was applied separately within each conception-group comparison (IVF vs. NC and ICSI vs. NC) and each outcome: across 287,027 CpGs for the EWAS, across 25 DMRs for mean methylation, and across 24 DMRs for epipolymorphism. We denote the resulting adjusted p-values as FDR and used FDR < 0.05 as the significance threshold. The same regional families were used within each sensitivity analysis. As a sensitivity analysis of multiplicity, the two comparisons were combined into 50 mean-methylation tests and 48 epipolymorphism tests; Bonferroni correction was also examined for the 50 mean-methylation tests.

3. Results

3.1. Characteristics of the Study Participants

The characteristics of the 87 newborns included in the final analysis (29 per group) are summarized in Table 1. There were no significant differences in gestational age at delivery, birth weight, offspring sex distribution, maternal age at delivery, or paternal age at delivery among the three groups.

Maternal pre-pregnancy BMI was significantly lower in the IVF group than in the NC group (NC: 20.7 ± 1.0, IVF: 19.7 ± 1.7, $p = 0.021$, ICSI: 20.4 ± 1.3, $p = 0.414$). In addition, the proportion of primiparous women was significantly higher in the IVF and ICSI groups than in the NC group (NC: 13/29, IVF: 26/29, $p < 0.001$; ICSI: 22/29, $p = 0.018$).

3.2. Between-Group Comparison of Genome-Wide DNA Methylation Status

To assess the quality of the RRBS data, we calculated the CpG coverage profile of each sample using the Read Count quantitation in SeqMonk and computed Pearson correlation coefficients across all 90 samples. The exclusion threshold (mean intersample correlation < 0.8) was defined before any group comparison. The overall mean intersample Pearson correlation was 0.87. Control_16, IVF_5, and ICSI_16 had mean correlations of 0.55, 0.79, and 0.75, respectively (Figure 2). Requiring coverage of at least 20 reads in every sample yielded 58,862 CpGs when all 90 samples were included and 287,027 CpGs after exclusion of these three samples. The three samples were excluded to retain broader shared genomic coverage, leaving 87 samples for the primary analyses (Figure 1).

The genomic inflation factors were 1.019 for IVF and 1.021 for ICSI, indicating little overall inflation in the test statistics (Figure 3A). No CpG reached the genome-wide significance threshold after Benjamini–Hochberg correction (adjusted $p < 0.05$) in either comparison (Figure 3B).

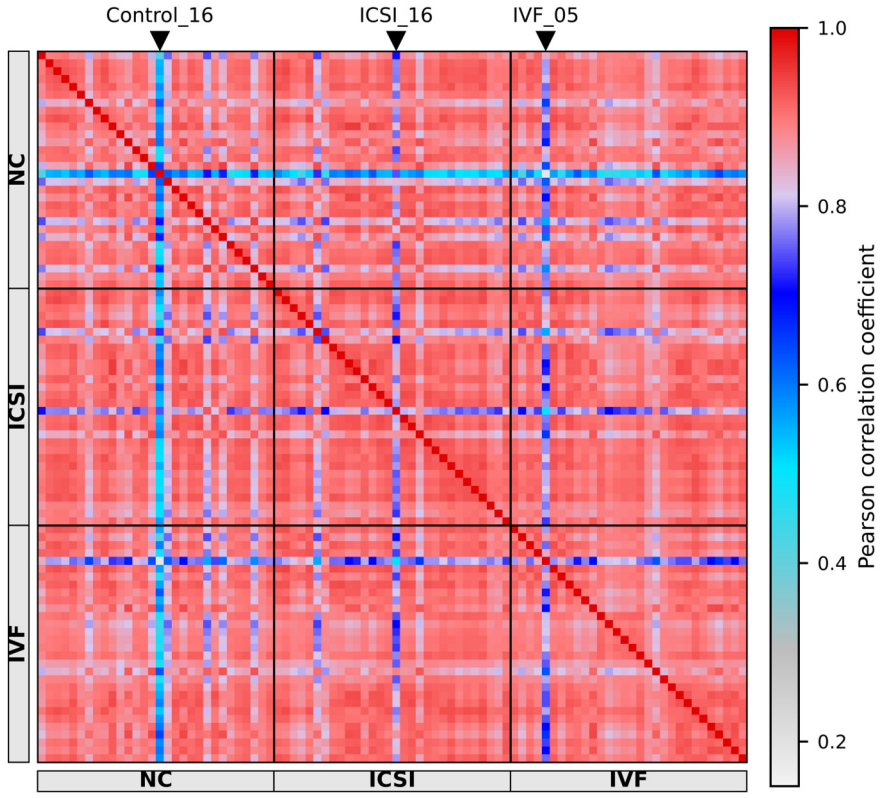

Figure 2. Heatmap of pairwise Pearson correlation coefficients based on CpG coverage profiles. CpG coverage profiles for each sample were calculated using the Read Count quantitation pipeline of SeqMonk, and pairwise Pearson correlation coefficients were estimated across all 90 samples. The color scale indicates the correlation coefficients, with red representing a correlation of 1, and transitioning through blue and light blue to gray as the value approaches 0. The overall mean correlation coefficient was 0.87. Black arrowheads indicate the three samples with mean intersample correlations below 0.8 that were excluded from the primary analyses; the rationale for exclusion and other available sequencing-quality measures are described in the text and Table S1.

3.3. Between-Group Comparison of DNA Methylation Levels at Imprinted DMRs

In the primary analysis, no DMR reached FDR < 0.05 in the IVF comparison. In the ICSI comparison, weighted mean methylation at PRR25_1 was lower than in NC (adjusted difference, −13.0 percentage points; 95% CI, −19.7 to −6.4; FDR < 0.01; Figure 4).

Residual diagnostics did not indicate problems that would affect the main finding. Departures from normality were observed at 6 (ICSI) and 8 (IVF) of the 25 DMRs, mainly as left-skewed residuals at DMRs with methylation close to 100% (Figure S1), and heteroscedasticity at 3 (ICSI) and 2 (IVF) DMRs; neither was observed for PRR25_1. No observation had a Cook's distance > 1 (maximum, 0.34 for ICSI and 0.46 for IVF) (Table S4).

The ICSI association remained negative and significant in sensitivity analyses using HC3 standard errors, influential-observation exclusion, quasi-binomial models, and additional adjustment for depth, library preparation batch, or sequencing run (estimates, −16.1 to −11.9 percentage points; FDR < 0.05; Table S5). Leave-one-out estimates ranged from −14.5 to −12.2 percentage points (all nominal $p \leq 6.4 \times 10^{-4}$; Table S5). Direct correction for estimated bisulfite non-conversion retained the ICSI–NC association at PRR25_1 (−13.1 percentage points; FDR = 0.006). With additional adjustment for CHH methylation as a covariate, the estimate remained negative but did not meet the FDR threshold (−11.2 percentage points; nominal $p = 0.002$; FDR = 0.053; Tables S5 and S6).

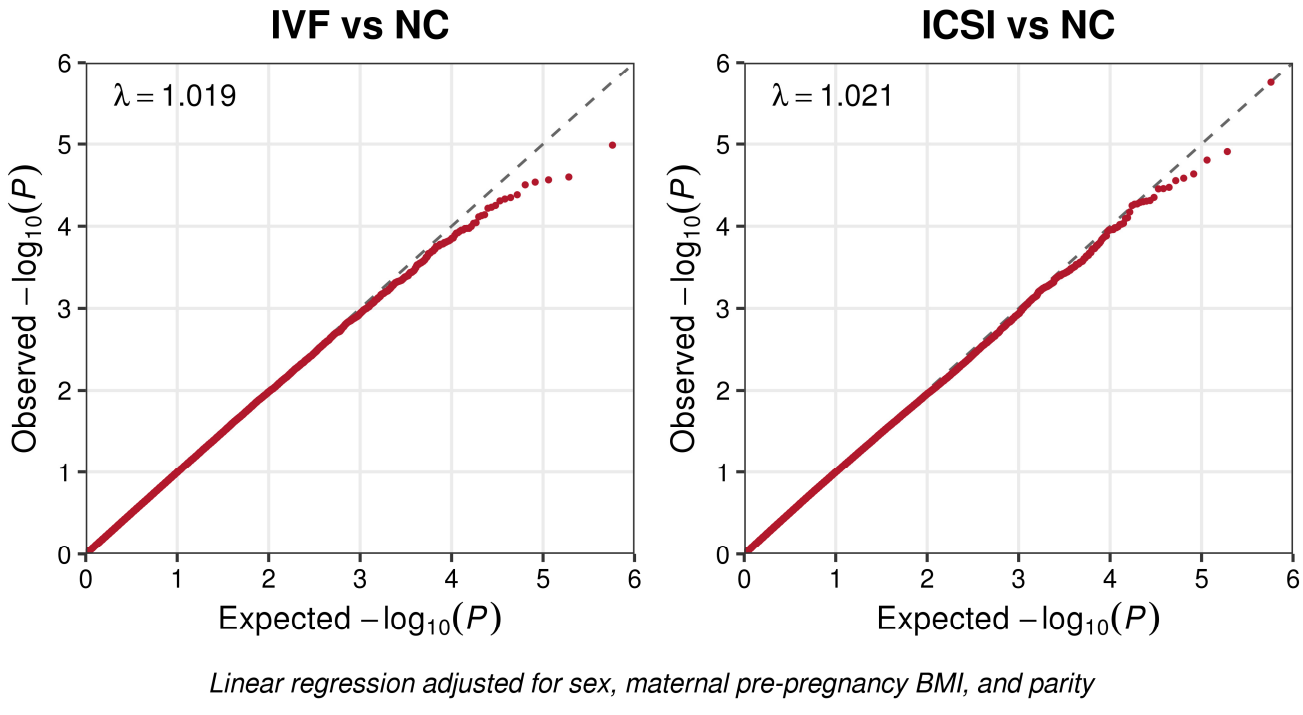

(**A**)

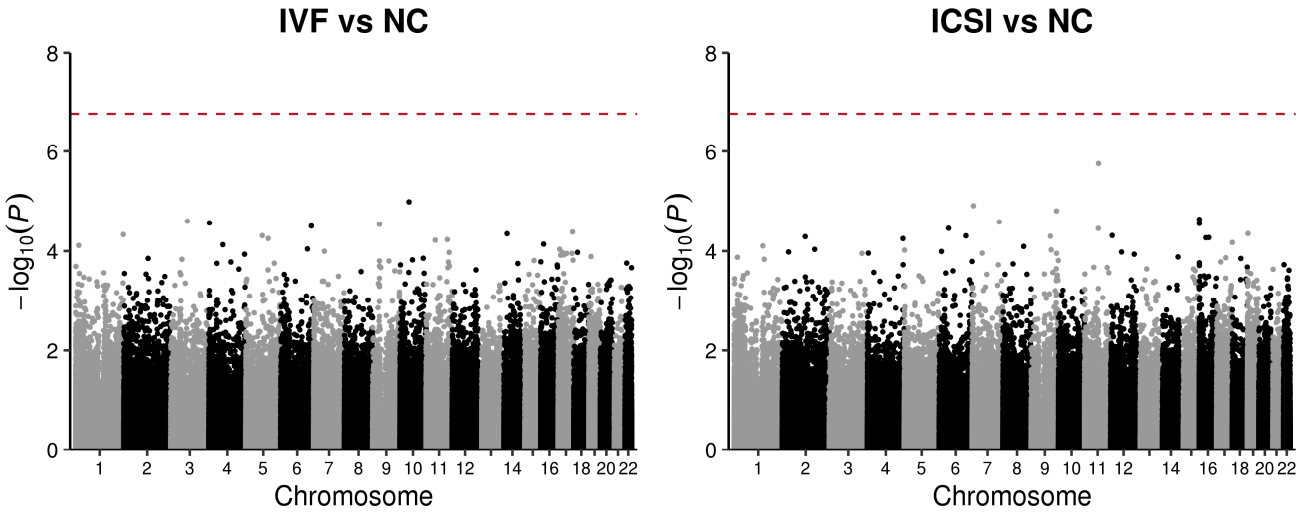

(**B**)

Figure 3. (**A**) Quantile–Quantile plots of observed versus expected $-\log_{10}(p)$ values from the EWAS of ART. The observed $-\log_{10}(p)$ values on the y-axis were derived from epigenome-wide association studies on IVF (left) and ICSI (right) using linear regression models adjusting for offspring sex, pre-pregnancy BMI, and parity. The expected $-\log_{10}(p)$ values on the x-axis represent the theoretical distribution under the null hypothesis for the 287,027 CpG sites tested. The genomic inflation factor lambda calculated from these p values is indicated in the bottom right corner of each plot. (**B**), Manhattan plots of EWAS results of ART cases. Manhattan plots of results from analysis of epigenome-wide association studies on IVF (left) and ICSI (right) using linear regression models adjusting for offspring sex, pre-pregnancy BMI, and parity. The x-axis shows the chromosomal position, and the y-axis shows the $-\log_{10}(p)$ values of the IVF and ICSI associations. The horizontal red line corresponds to a false discovery rate (FDR) threshold of 0.05.

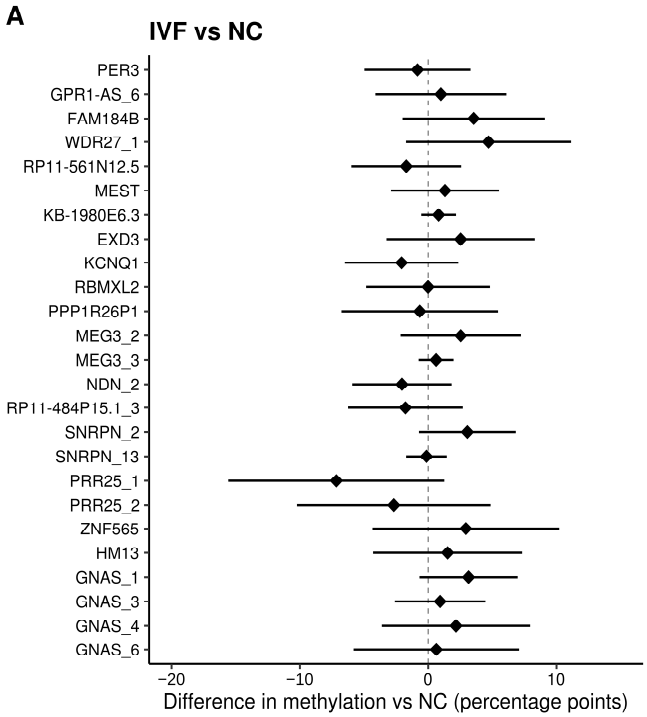

	COE	95% CI	*p.val*	FDR
PER3	−0.8	−5.0, 3.3	0.686	0.833
GPR1-AS_6	1.0	−4.1, 6.1	0.699	0.833
FAM184B	3.5	−2.0, 9.1	0.205	0.748
WDR27_1	4.7	−1.7, 11.1	0.149	0.748
RP11-561N12.5	−1.7	−6.0, 2.6	0.426	0.748
MEST	1.3	−2.9, 5.5	0.536	0.788
KB-1980E6.3	0.8	−0.5, 2.2	0.234	0.748
EXD3	2.5	−3.3, 8.3	0.384	0.748
KCNQ1	−2.1	−6.5, 2.3	0.351	0.748
RBMXL2	0.0	−4.8, 4.8	0.996	0.996
PPP1R26P1	−0.7	−6.8, 5.4	0.829	0.899
MEG3_2	2.5	−2.2, 7.2	0.283	0.748
MEG3_3	0.6	−0.7, 2.0	0.369	0.748
NDN_2	−2.0	−5.9, 1.8	0.294	0.748
RP11-484P15.1_3	−1.8	−6.2, 2.7	0.430	0.748
SNRPN_2	3.1	−0.7, 6.8	0.111	0.748
SNRPN_13	−0.1	−1.7, 1.4	0.863	0.899
PRR25_1	−7.2	−15.6, 1.3	0.094	0.748
PRR25_2	−2.7	−10.2, 4.9	0.479	0.748
ZNF565	2.9	−4.3, 10.2	0.422	0.748
HM13	1.5	−4.3, 7.3	0.604	0.795
GNAS_1	3.1	−0.7, 7.0	0.105	0.748
GNAS_3	0.9	−2.6, 4.5	0.601	0.795
GNAS_4	2.2	−3.6, 7.9	0.456	0.748
GNAS_6	0.6	−5.8, 7.1	0.845	0.899

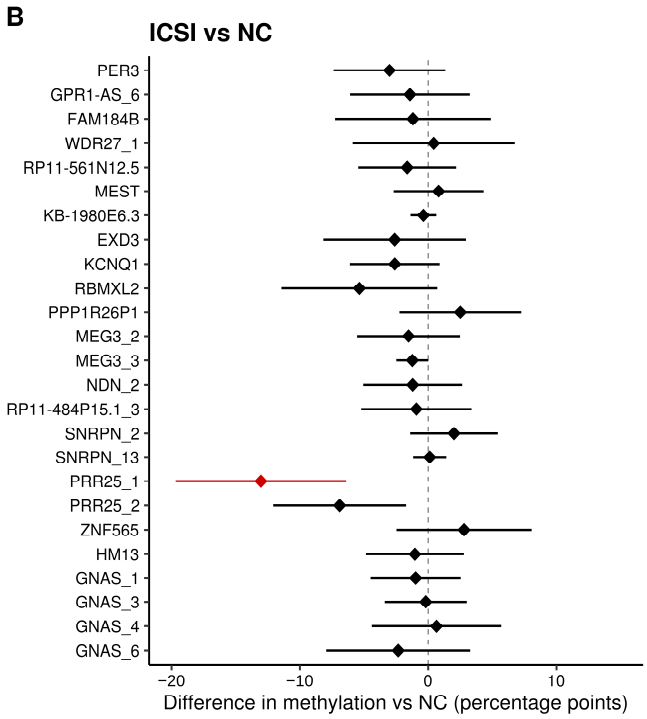

	COE	95% CI	*p.val*	FDR
PER3	−3.0	−7.4, 1.3	0.170	0.710
GPR1-AS_6	−1.4	−6.1, 3.2	0.543	0.817
FAM184B	−1.2	−7.3, 4.9	0.696	0.828
WDR27_1	0.4	−5.9, 6.7	0.892	0.906
RP11-561N12.5	−1.6	−5.5, 2.2	0.393	0.817
MEST	0.8	−2.7, 4.3	0.644	0.828
KB-1980E6.3	−0.4	−1.4, 0.6	0.462	0.817
EXD3	−2.6	−8.2, 2.9	0.350	0.817
KCNQ1	−2.6	−6.1, 0.9	0.141	0.705
RBMXL2	−5.4	−11.4, 0.7	0.082	0.514
PPP1R26P1	2.5	−2.2, 7.3	0.295	0.817
MEG3_2	−1.5	−5.5, 2.5	0.447	0.817
MEG3_3	−1.2	−2.5, 0.0	0.052	0.434
NDN_2	−1.2	−5.1, 2.6	0.532	0.817
RP11-484P15.1_3	−0.9	−5.2, 3.4	0.669	0.828
SNRPN_2	2.0	−1.4, 5.4	0.243	0.817
SNRPN_13	0.1	−1.2, 1.4	0.853	0.906
PRR25_1	**−13.0**	**−19.7, −6.4**	**<0.001**	**0.006***
PRR25_2	−6.9	−12.1, −1.7	0.010	0.124
ZNF565	2.8	−2.5, 8.1	0.292	0.817
HM13	−1.0	−4.9, 2.8	0.588	0.817
GNAS_1	−1.0	−4.5, 2.5	0.578	0.817
GNAS_3	−0.2	−3.4, 3.0	0.906	0.906
GNAS_4	0.6	−4.4, 5.7	0.798	0.906
GNAS_6	−2.3	−8.0, 3.3	0.407	0.817

Figure 4. Regression coefficient for the NC–IVF and NC-ICSI difference in DNA methylation. (**A**) The forest plot illustrates the coefficients (COE) and 95% confidence intervals (CIs) derived from multiple linear regression analysis for the IVF group compared to the natural conception (NC) group. (**B**) The forest plot illustrates the coefficients (COE) and 95% confidence intervals (CIs) derived from multiple linear regression analysis for the ICSI group compared to the natural conception (NC) group. The exact numerical values for the COE, 95% CI, *p*-value, and false discovery rate (FDR) are provided for each region. Asterisks indicate statistical significance ($p < 0.05$ and FDR < 0.05). Significant values are highlighted in bold red. Models were adjusted for infant sex (male or female), maternal parity (primiparous or multiparous), and pre-pregnancy BMI.

For IVF, PRR25_1 reached FDR < 0.05 only after exclusion of influential observations (#2 in Table S6; −13.5 percentage points, FDR = 0.019). This result was not consistent across the other analyses and was not interpreted as a robust association.

The ICSI–NC difference in PRR25_1 methylation remained negative after adjustment for library preparation batch (#5 in Table S6; −11.9 percentage points, FDR = 0.009) and sequencing run (#5b in Table S6; −12.5 percentage points, FDR = 0.003). In the IVF comparison restricted to shared runs, the estimate was −14.1 percentage points (nominal $p = 0.013$, FDR = 0.24; $n = 30$; Table S6). All 11 CpGs within PRR25_1 showed lower methylation in the ICSI comparison (estimated differences, −17.6 to −8.2 percentage points; nominal $p < 0.05$ at each site; Table S6).

The Sino-mQTL database [27] search did not identify a reported association for the queried CpGs in PRR25_1. This annotation does not exclude genetic influences on methylation measurements or regulation.

3.4. Between-Group Comparison of Imprinted DMRs Focusing on Epiallele Diversity

Next, to evaluate the diversity of methylation patterns within loci, which is difficult to detect by comparing mean methylation levels between groups, we analyzed epipolymorphism, an index of epiallele diversity. Epipolymorphism is an index calculated from the distribution of methylated/unmethylated patterns within the same 4-CpG block; lower values indicate more homogeneous patterns, whereas higher values indicate greater diversity [10] (Figure 5).

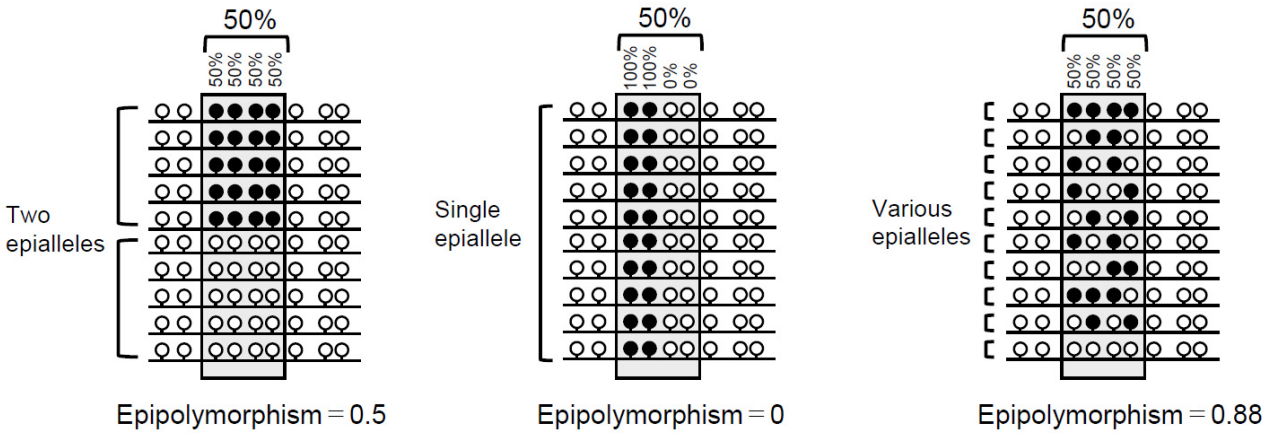

Figure 5. Average methylation level cannot distinguish epiallelic diversity. Schematic illustration of methylated and unmethylated cytosines, shown as closed and open circles, respectively. Although the average DNA methylation level within each gray-shaded region is identical at 50%, the underlying epiallelic patterns differ among these conceptual examples and cannot be distinguished by average methylation level alone. Epipolymorphism analysis, which quantifies epiallele diversity, can capture these differences; more homogeneous epiallele compositions yield lower epipolymorphism values. This figure was adapted from [10].

No DMR reached FDR < 0.05 for epipolymorphism in the primary analysis of 24 DMRs. In the IVF comparison, KB-1980E6.3, MEG3_2, and HM13 showed nominal decreases, and RP11-484P15.1_3 showed a nominal increase ($p < 0.05$). In the ICSI comparison, PRR25_1 showed a nominal decrease (−0.150; 95% CI, −0.252 to −0.047; $p = 0.005$), which did not remain significant after BH correction (Figure 6).

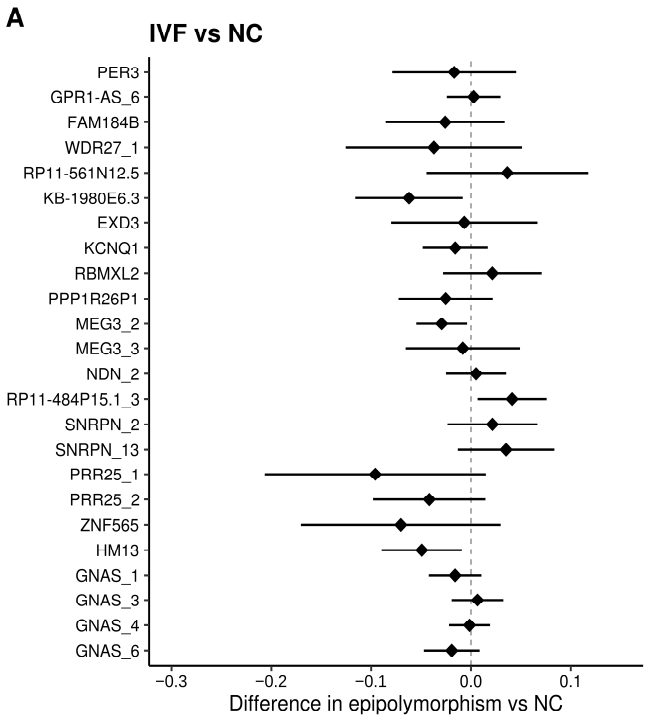

	COE	95% CI	*p.val*	FDR
PER3	−0.017	−0.079, 0.045	0.589	0.778
GPR1-AS_6	0.003	−0.024, 0.030	0.842	0.888
FAM184B	−0.026	−0.085, 0.034	0.388	0.568
WDR27_1	−0.037	−0.126, 0.051	0.402	0.568
RP11-561N12.5	0.036	−0.045, 0.118	0.371	0.568
KB-1980E6.3	−0.062	−0.116, −0.008	0.025	0.148
EXD3	−0.007	−0.080, 0.067	0.855	0.888
KCNQ1	−0.016	−0.048, 0.017	0.336	0.568
RBMXL2	0.021	−0.028, 0.071	0.389	0.568
PPP1R26P1	−0.025	−0.073, 0.022	0.286	0.568
MEG3_2	−0.029	−0.055, −0.004	0.025	0.148
MEG3_3	−0.008	−0.065, 0.049	0.775	0.885
NDN_2	0.005	−0.025, 0.035	0.736	0.883
RP11-484P15.1_3	0.041	0.007, 0.076	0.020	0.148
SNRPN_2	0.022	−0.024, 0.067	0.343	0.568
SNRPN_13	0.035	−0.013, 0.084	0.151	0.459
PRR25_1	−0.096	−0.207, 0.015	0.088	0.425
PRR25_2	−0.042	−0.098, 0.014	0.142	0.459
ZNF565	−0.070	−0.170, 0.030	0.164	0.459
HM13	−0.049	−0.089, −0.009	0.017	0.148
GNAS_1	−0.016	−0.042, 0.010	0.231	0.555
GNAS_3	0.007	−0.019, 0.032	0.616	0.778
GNAS_4	−0.001	−0.022, 0.019	0.888	0.888
GNAS_6	−0.019	−0.047, 0.009	0.172	0.459

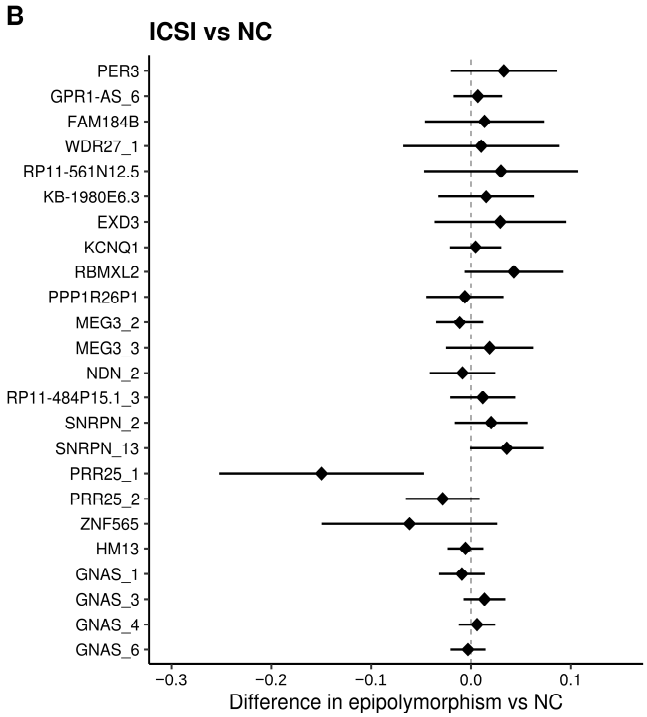

	COE	95% CI	*p.val*	FDR
PER3	0.033	−0.020, 0.086	0.220	0.756
GPR1-AS_6	0.007	−0.018, 0.031	0.577	0.765
FAM184B	0.014	−0.046, 0.073	0.651	0.781
WDR27_1	0.010	−0.068, 0.089	0.794	0.794
RP11-561N12.5	0.030	−0.047, 0.107	0.438	0.764
KB-1980E6.3	0.015	−0.033, 0.063	0.528	0.764
EXD3	0.029	−0.037, 0.095	0.376	0.764
KCNQ1	0.005	−0.021, 0.030	0.723	0.786
RBMXL2	0.043	−0.006, 0.092	0.087	0.694
PPP1R26P1	−0.006	−0.045, 0.033	0.753	0.786
MEG3_2	−0.011	−0.035, 0.012	0.342	0.764
MEG3_3	0.019	−0.025, 0.063	0.396	0.764
NDN_2	−0.009	−0.041, 0.024	0.606	0.765
RP11-484P15.1_3	0.012	−0.021, 0.045	0.472	0.764
SNRPN_2	0.020	−0.016, 0.057	0.273	0.764
SNRPN_13	0.036	−0.001, 0.073	0.056	0.672
PRR25_1	−0.150	−0.252, −0.047	0.005	0.121
PRR25_2	−0.028	−0.065, 0.009	0.130	0.756
ZNF565	−0.062	−0.150, 0.026	0.166	0.756
HM13	−0.006	−0.024, 0.012	0.541	0.764
GNAS_1	−0.009	−0.032, 0.014	0.431	0.764
GNAS_3	0.014	−0.007, 0.035	0.202	0.756
GNAS_4	0.006	−0.012, 0.024	0.512	0.764
GNAS_6	−0.003	−0.021, 0.015	0.733	0.786

Figure 6. Regression coefficient for the NC–IVF and NC-ICSI difference in epipolymorphism. (**A**) The forest plot illustrates the coefficients (COE) and 95% confidence intervals (CIs) derived from multiple linear regression analysis comparing the IVF group to the natural conception group. (**B**) The forest plot illustrates the coefficients (COE) and 95% confidence intervals (CIs) derived from multiple linear regression analysis comparing the ICSI group to the natural conception group. The exact numerical values for the COE, 95% CI, *p*-value, and false discovery rate (FDR) are provided for each region. Asterisks indicate statistical significance ($p < 0.05$ and FDR < 0.05). Significant values are highlighted in bold red. Models were adjusted for infant sex (male or female), maternal parity (primiparous or multiparous), and pre-pregnancy BMI.

Sensitivity analyses did not provide consistent evidence of an epipolymorphism association. PRR25_1 reached FDR < 0.05 after influential-observation exclusion (#2 in Table S7; ICSI, −0.197, FDR = 0.003; IVF, −0.190, FDR = 0.005). SNRPN_13 reached this threshold in a model additionally including mean methylation (#6 in Table S7; ICSI, +0.039, FDR = 0.02, #6b in Table S7; ICSI, +0.040, FDR = 0.016). These findings were specific to individual sensitivity analyses.

At PRR25_1, epipolymorphism was strongly correlated with mean methylation (r = 0.95). When mean methylation was included as a linear covariate, the ICSI coefficient changed to +0.042 (#6 in Table S7; 95% CI, 0.007 to 0.077; nominal $p = 0.019$). With linear and quadratic methylation terms, the coefficient was +0.007 (#6b in Table S7; 95% CI, −0.012 to 0.025; $p = 0.47$). Thus, the negative ICSI association was not maintained in these conditional models, and the adjusted estimates depended on the model specification.

For the epipolymorphism findings shown in Figure 6, we also searched the Sino-mQTL database [27] for the relevant CpGs. No reported mQTL associations were identified for the queried CpGs; however, this does not exclude genetic influences on these findings.

4. Discussion

This study applied epipolymorphism analysis to complement mean-based assessment of DNA methylation in cord blood from newborns conceived through ART. No individual CpG reached the FDR threshold in the EWAS. The genomic inflation factors were close to 1, indicating little overall inflation in the test statistics. Previous studies of assisted conception have reported varying methylation findings, including a small number of associated CpGs in a multi-cohort meta-analysis [7] and more widespread differences in another cohort [28]. Our nonsignificant EWAS findings do not exclude smaller associations that this study had limited power to detect. Developmental selection could also influence which epigenetic alterations are represented among liveborn children. However, we did not study embryos or pregnancy losses and could not evaluate this possibility.

To examine locus-specific methylation, we analyzed 25 predefined imprinted DMRs with sufficient RRBS coverage. These regions were selected independently of the EWAS findings. ICSI was associated with lower weighted mean methylation at PRR25_1, and this association remained significant in most sensitivity analyses. PRR25 has been described as a maternally methylated DMR with paternal expression and tissue-specific methylation characteristics [29–31]. Lower methylation at this region has also been reported in relation to ART conception [28] and increasing parental age [32]. These observations provide context for the present association but do not establish that it results from the ART procedure or represents disrupted imprinting. Independent validation remains necessary.

Epipolymorphism summarizes the distribution of methylation patterns across reads within a CpG block. It provides a complementary description because the same mean methylation level can arise from different pattern distributions, as illustrated in Figure 5. Our application extends the assessment of ART-associated methylation variation to this additional dimension, without establishing greater sensitivity than mean-based analysis.

No epipolymorphism difference remained significant after FDR correction in the primary analysis. At PRR25_1, epipolymorphism was strongly correlated with mean methylation (r = 0.95), and the nominal negative association with ICSI was not preserved after adjustment for mean methylation. These conditional analyses do not demonstrate a separate biological process or establish that the original association was entirely attributable to the mean. Rather, the results highlight the need to interpret methylation-pattern diversity together with mean methylation. The nominal increases and decreases at other loci cannot be distinguished from sampling variation in this dataset.

In the primary analysis, the PRR25 methylation association was significant for ICSI but not for IVF; this does not establish a difference between the procedures, which was not tested directly. The groups also differed in clinical background, and parental infertility or other factors could contribute to the observed association. Consequently, the present comparisons cannot isolate the causal effect of the ART procedure. Even after multiple-testing correction, the possibility of a false-positive association remains.

Umbilical cord blood allowed us to assess neonatal methylation patterns with limited influence from postnatal exposures. The measurements represent a mixture of blood cell types and do not characterize methylation in other tissues. Placenta-specific changes were outside the scope of this study.

This study has several limitations. First, with 29 participants per group, the precision and power to detect small associations were limited. The magnitude of the PRR25 association may be overestimated and requires independent validation. Second, the selected newborns do not represent the full range of outcomes following ART, including pregnancies that did not result in live birth. The persistence and clinical consequences of the observed methylation differences were not evaluated. Third, blood cell composition could not be reliably estimated from the available RRBS coverage of the selected reference markers. The analyses were not adjusted for cell composition, and both mean methylation and epipolymorphism may reflect differences in the mixture of cells rather than variation within a particular cell type.

Residual confounding by parental infertility and other clinical factors also remains possible. Fifteen of the 29 IVF samples were sequenced in a run without NC samples, limiting the separation of group and sequencing-run effects in the IVF comparison. The PRR25 finding has not been confirmed using technical replicates, an independent assay, or an independent cohort. Without genotype data, CpG-disrupting variants, alignment effects, and other genetic influences cannot be excluded.

Finally, the epipolymorphism analysis was limited to 137 qualifying four-CpG blocks in 24 DMRs, with few blocks in some regions and incomplete sample availability at five DMRs. Regional summaries may therefore depend on which blocks are covered in each sample. Pooled reads do not identify parental alleles or individual cell types, and epipolymorphism should be interpreted alongside mean methylation. Larger independent studies and complementary measurements are needed to assess reproducibility. Long-read methylation sequencing could extend the assessment to longer methylation patterns, but would not by itself resolve confounding or establish clinical relevance.

5. Conclusions

In this exploratory study, no individual CpG reached the significance threshold in the EWAS, whereas ICSI was associated with lower mean methylation at PRR25 after FDR correction. This association remained significant in most sensitivity analyses but requires independent validation. No epipolymorphism difference remained significant after FDR correction in the primary analysis, and the nominal difference at PRR25 did not establish a change independent of mean methylation. By assessing methylation-pattern diversity alongside mean methylation, this study provides a complementary description of neonatal cord-blood methylation for future studies of ART and other exposures. Larger independent studies are needed to establish the reproducibility and biological and clinical significance of the findings.

Supplementary Materials: The following supporting information can be downloaded at: https://www.mdpi.com/article/10.3390/biom16121711/s1, Table S1: Sequencing, alignment and bisulfite conversion metrics of the 90 RRBS libraries; Table S2: Sequencing depth, mapping efficiency, bisulfite conversion efficiency, insert size and read coverage by conception group, library preparation

set and sequencing run; Table S3: Genomic loci of the imprinted DMRs analyzed for mean-based methylation and epipolymorphism, and the individual methylated CpGs mapped to each DMR; Table S4: Regression diagnostics of the primary models for weighted mean methylation at 25 imprinted DMRs; Table S5: Sensitivity analyses of the association between conception method and weighted mean methylation at PRR25_1; Table S6: Results of the primary and sensitivity analyses of weighted mean methylation at 25 imprinted DMRs; Table S7: Results of the primary and sensitivity analyses of weighted mean epipolymorphism at 24 imprinted DMRs; Figure S1: Normal Q–Q plots of standardized residuals from the primary regression models for weighted mean methylation at the 25 imprinted DMRs.

Author Contributions: Conceptualization, Data curation, and Writing—original draft, K.H.; Investigation, M.Y., K.T., T.K. and K.N.; Supervision and Writing—review and editing, K.T. and O.S. All authors contributed to Data curation and Writing—review and editing and approved the final version. All authors have read and agreed to the published version of the manuscript.

Funding: The research was funded by JSPS KAKENHI Grant Number 24K02415, the Practical Research Project for Rare/Intractable Diseases of the Japan Agency for Medical Research and Development (AMED) under Grant Number 26ek0109879s0201/26ek0109879h0001, Gunma University for the promotion of scientific research (G2). The funders had no role in the study design, sample collection, data analysis, interpretation of the results, manuscript preparation or decision to submit the article for publication.

Institutional Review Board Statement: This study was approved by the Ethics Committee of the National Center for Child Health and Development (approval no. 234, 11 July 2007) and all participants received an oral explanation of the study and provided written informed consent. The study was conducted in accordance with the principles of the Declaration of Helsinki.

Informed Consent Statement: Written informed consent was obtained from all adult participants following an in-person explanation of the study. For newborn participants, written informed consent was obtained from their parents on their behalf.

Data Availability Statement: The datasets generated and analysed during the current study are available in the ArrayExpress repository, accession code E-MTAB-17812 (www.ebi.ac.uk/arrayexpress/experiments/E-MTAB-17812/ (accessed on 17 November 2026)). The data will be made publicly available upon publication of this article. Other data underlying this article will be shared by the corresponding author upon reasonable request, subject to ethical and privacy restrictions.

Acknowledgments: The authors are grateful to all participating families who took part in this study. We also thank the clinical staff involved in sample collection and the laboratory staff who contributed to DNA preparation, RRBS library construction, sequencing and data processing at NCCHD.

Conflicts of Interest: The authors declare no conflicts of interest.

Abbreviations

The following abbreviations are used in this manuscript:

ART	Assisted Reproductive Technology
ICSI	Intracytoplasmic Sperm Injection
BMI	Body Mass Index
EWAS	Epigenome-wide Association Study
FDR	False Discovery Rate
IVF	In vitro Fertilization
NC	Natural Conception
RRBS	Reduced Representation Bisulfite Sequencing
WGBS	Whole-genome Bisulfite Sequencing

References

1. Faraji, J.; Metz, G.A.S. Environmental epigenetics: New horizons in redefining biological and health outcomes. *Environ. Int.* **2026**, *208*, 110072. [CrossRef] [PubMed]

2. Cortessis, V.K.; Azadian, M.; Buxbaum, J.; Sanogo, F.; Song, A.Y.; Sriprasert, I.; Wei, P.C.; Yu, J.; Chung, K.; Siegmund, K.D. Comprehensive meta-analysis reveals association between multiple imprinting disorders and conception by assisted reproductive technology. *J. Assist. Reprod. Genet.* **2018**, *35*, 943–952. [CrossRef] [PubMed]
3. Lazaraviciute, G.; Kauser, M.; Bhattacharya, S.; Haggarty, P.; Bhattacharya, S. A systematic review and meta-analysis of DNA methylation levels and imprinting disorders in children conceived by IVF/ICSI compared with children conceived spontaneously. *Hum. Reprod. Update* **2014**, *20*, 840–852. [CrossRef] [PubMed]
4. Peña, C.J. Epigenetic regulation of brain development, plasticity, and response to early-life stress. *Neuropsychopharmacology* **2026**, *51*, 5–15. [CrossRef] [PubMed]
5. El Hajj, N.; Haertle, L.; Dittrich, M.; Denk, S.; Lehnen, H.; Hahn, T.; Schorsch, M.; Haaf, T. DNA methylation signatures in cord blood of ICSI children. *Hum. Reprod.* **2017**, *32*, 1761–1769. [CrossRef] [PubMed]
6. Yeung, E.H.; Mendola, P.; Sundaram, R.; Zeng, X.; Guan, W.; Tsai, M.Y.; Robinson, S.L.; Stern, J.E.; Ghassabian, A.; Lawrence, D.; et al. Conception by fertility treatment and offspring deoxyribonucleic acid methylation. *Fertil. Steril.* **2021**, *116*, 493–504. [CrossRef] [PubMed]
7. Caramaschi, D.; Jungius, J.; Page, C.M.; Novakovic, B.; Saffery, R.; Halliday, J.; Lewis, S.; Magnus, M.C.; London, S.J.; Håberg, S.E.; et al. Association of medically assisted reproduction with offspring cord blood DNA methylation across cohorts. *Hum. Reprod.* **2021**, *36*, 2403–2413. [CrossRef] [PubMed]
8. Novakovic, B.; Lewis, S.; Halliday, J.; Kennedy, J.; Burgner, D.P.; Czajko, A.; Kim, B.; Sexton-Oates, A.; Juonala, M.; Hammarberg, K.; et al. Assisted reproductive technologies are associated with limited epigenetic variation at birth that largely resolves by adulthood. *Nat. Commun.* **2019**, *10*, 3922. [CrossRef] [PubMed]
9. Tobi, E.W.; Almqvist, C.; Hedman, A.; Andolf, E.; Holte, J.; Olofsson, J.I.; Wramsby, H.; Wramsby, M.; Pershagen, G.; Heijmans, B.T.; et al. DNA methylation differences at birth after conception through ART. *Hum. Reprod.* **2021**, *36*, 248–259. [CrossRef] [PubMed]
10. Landan, G.; Cohen, N.M.; Mukamel, Z.; Bar, A.; Molchadsky, A.; Brosh, R.; Horn-Saban, S.; Zalcenstein, D.A.; Goldfinger, N.; Zundelevich, A.; et al. Epigenetic polymorphism and the stochastic formation of differentially methylated regions in normal and cancerous tissues. *Nat. Genet.* **2012**, *44*, 1207–1214. [CrossRef] [PubMed]
11. Chen, X.; Ashoor, H.; Musich, R.; Wang, J.; Zhang, M.; Zhang, C.; Lu, M.; Li, S. epihet for intra-tumoral epigenetic heterogeneity analysis and visualization. *Sci. Rep.* **2021**, *11*, 376. [CrossRef] [PubMed]
12. Boyle, P.; Clement, K.; Gu, H.; Smith, Z.D.; Ziller, M.; Fostel, J.L.; Holmes, L.; Meldrim, J.; Kelley, F.; Gnirke, A.; et al. Gel-free multiplexed reduced representation bisulfite sequencing for large-scale DNA methylation profiling. *Genome Biol.* **2012**, *13*, R92. [CrossRef] [PubMed]
13. Gu, H.; Smith, Z.D.; Bock, C.; Boyle, P.; Gnirke, A.; Meissner, A. Preparation of reduced representation bisulfite sequencing libraries for genome-scale DNA methylation profiling. *Nat. Protoc.* **2011**, *6*, 468–481. [CrossRef] [PubMed]
14. Nakabayashi, K.; Yamamura, M.; Haseagawa, K.; Hata, K. Reduced Representation Bisulfite Sequencing (RRBS). *Methods Mol. Biol.* **2023**, *2577*, 39–51. [CrossRef] [PubMed]
15. Krueger, F.; Andrews, S.R. Bismark: A flexible aligner and methylation caller for Bisulfite-Seq applications. *Bioinformatics* **2011**, *27*, 1571–1572. [CrossRef] [PubMed]
16. Langmead, B.; Salzberg, S.L. Fast gapped-read alignment with Bowtie 2. *Nat. Methods* **2012**, *9*, 357–359. [CrossRef] [PubMed]
17. Houseman, E.A.; Kile, M.L.; Christiani, D.C.; Ince, T.A.; Kelsey, K.T.; Marsit, C.J. Reference-free deconvolution of DNA methylation data and mediation by cell composition effects. *BMC Bioinform.* **2016**, *17*, 259. [CrossRef] [PubMed]
18. De Ridder, K.; Che, H.; Leroy, K.; Thienpont, B. Benchmarking of methods for DNA methylome deconvolution. *Nat. Commun.* **2024**, *15*, 4134. [CrossRef] [PubMed]
19. Laajala, E.; Kalim, U.U.; Grönroos, T.; Rasool, O.; Halla-Aho, V.; Konki, M.; Kattelus, R.; Mykkänen, J.; Nurmio, M.; Vähä-Mäkilä, M.; et al. Umbilical cord blood DNA methylation in children who later develop type 1 diabetes. *Diabetologia* **2022**, *65*, 1534–1540. [CrossRef] [PubMed]
20. Akalin, A.; Kormaksson, M.; Li, S.; Garrett-Bakelman, F.E.; Figueroa, M.E.; Melnick, A.; Mason, C.E. methylKit: A comprehensive R package for the analysis of genome-wide DNA methylation profiles. *Genome Biol.* **2012**, *13*, R87. [CrossRef] [PubMed]
21. Kasuga, Y.; Kawai, T.; Miyakoshi, K.; Saisho, Y.; Tamagawa, M.; Hasegawa, K.; Ikenoue, S.; Ochiai, D.; Hida, M.; Tanaka, M.; et al. Epigenetic Changes in Neonates Born to Mothers With Gestational Diabetes Mellitus May Be Associated With Neonatal Hypoglycaemia. *Front. Endocrinol.* **2021**, *12*, 690648. [CrossRef] [PubMed]
22. Rakyan, V.K.; Down, T.A.; Balding, D.J.; Beck, S. Epigenome-wide association studies for common human diseases. *Nat. Rev. Genet.* **2011**, *12*, 529–541. [CrossRef] [PubMed]
23. Devlin, B.; Roeder, K. Genomic control for association studies. *Biometrics* **1999**, *55*, 997–1004. [CrossRef] [PubMed]
24. Zink, F.; Magnusdottir, D.N.; Magnusson, O.T.; Walker, N.J.; Morris, T.J.; Sigurdsson, A.; Halldorsson, G.H.; Gudjonsson, S.A.; Melsted, P.; Ingimundardottir, H.; et al. Insights into imprinting from parent-of-origin phased methylomes and transcriptomes. *Nat. Genet.* **2018**, *50*, 1542–1552. [CrossRef] [PubMed]

25. Li, S.; Garrett-Bakelman, F.; Perl, A.E.; Luger, S.M.; Zhang, C.; To, B.L.; Lewis, I.D.; Brown, A.L.; D'Andrea, R.J.; Ross, M.E.; et al. Dynamic evolution of clonal epialleles revealed by methclone. *Genome Biol.* **2014**, *15*, 472. [CrossRef]
26. Rossi, S.H.; Dombrowe, V.; Godfrey, L.; Bucaciuc Mracica, T.; Pita, S.; Milne-Clark, T.; Kyeremeh, J.; Park, G.; Smith, C.G.; Lach, R.P.; et al. Evidence of DNA methylation heterogeneity and epipolymorphism in kidney cancer tissue samples. *Oncogene* **2025**, *44*, 1024–1036. [CrossRef] [PubMed]
27. Peng, Q.; Liu, X.; Li, W.; Jing, H.; Li, J.; Gao, X.; Luo, Q.; Breeze, C.E.; Pan, S.; Zheng, Q.; et al. Analysis of blood methylation quantitative trait loci in East Asians reveals ancestry-specific impacts on complex traits. *Nat. Genet.* **2024**, *56*, 846–860. [CrossRef] [PubMed]
28. Håberg, S.E.; Page, C.M.; Lee, Y.; Nustad, H.E.; Magnus, M.C.; Haftorn, K.L.; Carlsen, E.Ø.; Denault, W.R.P.; Bohlin, J.; Jugessur, A.; et al. DNA methylation in newborns conceived by assisted reproductive technology. *Nat. Commun.* **2022**, *13*, 1896. [CrossRef] [PubMed]
29. Court, F.; Tayama, C.; Romanelli, V.; Martin-Trujillo, A.; Iglesias-Platas, I.; Okamura, K.; Sugahara, N.; Simón, C.; Moore, H.; Harness, J.V.; et al. Genome-wide parent-of-origin DNA methylation analysis reveals the intricacies of human imprinting and suggests a germline methylation-independent mechanism of establishment. *Genome Res.* **2014**, *24*, 554–569. [CrossRef] [PubMed]
30. Jadhav, B.; Monajemi, R.; Gagalova, K.K.; Ho, D.; Draisma, H.H.M.; van de Wiel, M.A.; Franke, L.; Heijmans, B.T.; van Meurs, J.; Jansen, R.; et al. RNA-Seq in 296 phased trios provides a high-resolution map of genomic imprinting. *BMC Biol.* **2019**, *17*, 50. [CrossRef] [PubMed]
31. Schulze, K.V.; Szafranski, P.; Lesmana, H.; Hopkin, R.J.; Hamvas, A.; Wambach, J.A.; Shinawi, M.; Zapata, G.; Carvalho, C.M.B.; Liu, Q.; et al. Novel parent-of-origin-specific differentially methylated loci on chromosome 16. *Clin. Epigenet.* **2019**, *11*, 60. [CrossRef] [PubMed]
32. Gao, C.; Amador, C.; Walker, R.M.; Campbell, A.; Madden, R.A.; Adams, M.J.; Bai, X.; Liu, Y.; Li, M.; Hayward, C.; et al. Phenome-wide analyses identify an association between the parent-of-origin effects dependent methylome and the rate of aging in humans. *Genome Biol.* **2023**, *24*, 117. [CrossRef] [PubMed]

Disclaimer/Publisher's Note: The statements, opinions and data contained in all publications are solely those of the individual author(s) and contributor(s) and not of MDPI and/or the editor(s). MDPI and/or the editor(s) disclaim responsibility for any injury to people or property resulting from any ideas, methods, instructions or products referred to in the content.